Biochem. J. (1987) 246, 455–465 (Printed in Great Britain)

Nitrogenase of *Klebsiella pneumoniae*

Kinetic studies on the Fe protein involving reduction by sodium dithionite, the binding of MgADP and a conformation change that alters the reactivity of the 4Fe–4S centre

Gillian A. ASHBY and Roger N. F. THORNELEY*
AFRC Unit of Nitrogen Fixation, University of Sussex, Falmer, Brighton BN1 9RQ, Sussex, U.K.

The kinetics of reduction of indigocarmine-dye-oxidized Fe protein of nitrogenase from *Klebsiella pneumoniae* ($Kp2_{ox}$) by sodium dithionite in the presence and absence of MgADP were studied by stopped-flow spectrophotometry at 23 °C and at pH 7.4. Highly co-operative binding of 2MgADP (composite $K > 4 \times 10^{10}$ M^{-2}) to $Kp2_{ox}$ induced a rapid conformation change which caused the redox-active 4Fe–4S centre to be reduced by $SO_2^{-\cdot}$ (formed by the predissociation of dithionite ion) with $k = 3 \times 10^6$ M$^{-1} \cdot$ s^{-1}. This rate constant is at least 30 times lower than that for the reduction of free $Kp2_{ox}$ ($k > 10^8$ M$^{-1} \cdot$ s^{-1}). Two mechanisms have been considered and limits obtained for the rate constants for MgADP binding/dissociation and a protein conformation change. Both mechanisms give rate constants (e.g. MgADP binding $3 \times 10^5 < k < 3 \times 10^6$ M$^{-1} \cdot$ s^{-1} and protein conformation change $6 \times 10^2 < k < 6 \times 10^3$ s^{-1}) that are similar to those reported for creatine kinase (EC 2.7.3.2). The kinetics also show that in the catalytic cycle of nitrogenase with sodium dithionite as reductant replacement of 2MgADP by 2MgATP occurs on reduced and not oxidized Kp2. Although the $Kp2_{ox}$ was reduced stoichiometrically by $SO_2^{-\cdot}$ and bound two equivalents of MgADP with complete conversion into the less-reactive conformation, it was only 45% active with respect to its ability to effect MgATP-dependent electron transfer to the MoFe protein.

INTRODUCTION

Klebsiella pneumoniae nitrogenase comprises two metalloproteins: the MoFe protein (Kp1) has an M_r of 218000 and contains 32 Fe and 2 Mo atoms and the Fe protein (Kp2) with an M_r of 68000 contains 4 Fe atoms. Nitrogenase catalyses the reduction of N_2 to $2NH_3$ with concomitant stoichiometric evolution of H_2. The eight-electron reduction cycle is coupled to the hydrolysis of 16 MgATP to yield 16 MgADP + 16 P_i [see Burgess (1985), Lowe *et al.* (1985), Orme-Johnson (1985), Stephens (1985) and Thorneley & Lowe (1985) for recent reviews of the structure and mechanism of nitrogenase action].

Thorneley & Lowe (1983) determined the rate constants that are sufficient to describe a single-electron-transfer cycle in which two equivalents of MgATP are hydrolysed (Scheme 1). The coupling of eight of these cycles formed the basis for their comprehensive mechanism of nitrogenase action (Lowe & Thorneley, 1984*a*,*b*; Thorneley & Lowe, 1984*a*,*b*). Thorneley & Lowe (1983) measured the rate of reduction of $Kp2_{ox}(MgADP)_2$ by $SO_2^{-\cdot}$ ($k_{+4} = 3 \times 10^6$ M$^{-1} \cdot$ s^{-1}). Their success in stimulating the dependence of H_2 evolution rates on $Na_2S_2O_4$ (sodium dithionite) concentration justified their assumption that this second-order rate constant dominated the kinetics of the reactions occurring in step 4 in Scheme 1. However, they did recognize the 'apparent' nature of k_{+4} inasmuch as step 4, Scheme 1, comprises several reactions. These include the dissociation of two equivalents of MgADP, followed by the association of two equivalents of MgATP to either $Kp2_{ox}$ or Kp2, the reduction by $SO_2^{-\cdot}$ of $Kp2_{ox}$, $Kp2_{ox}(MgADP)_2$, $Kp2_{ox}(MgATP)_2$ and possibly $Kp2_{ox}$(MgADP, MgATP). Several additional features further complicate a detailed kinetic analysis of these reactions. Kp2 and $Kp2_{ox}$ undergo MgATP- and MgADP-induced conformation changes, as was shown by changes in the symmetry of the e.p.r. feature at $g = 1.94$ for Kp2 (Lowe, 1978) and in the c.d. spectrum for $Kp2_{ox}$ (Stephens *et al.*, 1982). Further evidence for nucleotide-induced conformation changes in Kp2, Cp2 and Av2 is the increased sensitivity to O_2 inactivation (Smith *et al.*, 1976), altered reactivity of protein -SH groups (Thorneley & Eady, 1973; Walker & Mortenson, 1973; Hausinger & Howard, 1983) and increased rates of chelation of Fe by $\alpha\alpha$-bipyridyl or bathophenanthroline sulphonate (Walker & Mortenson, 1974; Ljones & Burris, 1978; Howard *et al.*, 1985). The midpoint potentials of Cp2 and Av2 become ~ 100 mV more negative when MgATP or MgADP bind (Zumft *et al.*, 1974; Watt, 1985; Morgan *et al.*, 1986).

The two e.p.r. signals associated with the reduced 4Fe–4S cluster in AV2 (Hagen *et al.*, 1985; Lindahl *et al.*, 1985; Watt & McDonald, 1985), Kp2 (D. J. Lowe, personal communication) and Cp2 (Morgan *et al.*, 1986) which arise from electron spin $S = 1/2$ and $S = 3/2$ systems are most likely associated with two conformation

Abbreviations used: the nitrogenase components of the various organisms are denoted by a capital letter indicating the genus and a lower-case letter indicating the species; the number 1 indicates the Mo,Fe-containing protein and the number 2 the Fe-containing protein: Kp, *Klebsiella pneumoniae*; Av, *Azotobacter vinelandii*; Ac, *Azotobacter chroococcum*; Cp, *Clostridium pasteurianum*. The subscript $_{ox}$ (e.g. $Kp2_{ox}$) indicates the oxidized species.

* To whom correspondence and reprint requests should be sent.

states of the protein. However the effect of MgATP and MgADP on the equilibrium between these conformation states is unclear (Hagen *et al.*, 1985; Morgan *et al.*, 1986).

An additional complication in kinetic analyses involving Kp2 is that Lowe & Thorneley (1984*a*,*b*) and Thorneley & Lowe (1984*a*,*b*) showed that Kp2 protein with a specific activity of ~ 1500 nmol of H_2 evolved·min^{-1}·mg of $protein^{-1}$ is only 40% active. The 60% of the protein that is inactive with respect to electron transfer to Kp1 is still capable of binding to Kp1 with kinetic constants characteristic of $Kp2_{ox}(MgADP)_2$. Although inactive with respect to electron transfer, this form of Kp2 is active in the sense that by binding to Kp1 it helps to suppress competing H_2 evolution and promotes N_2 reduction, particularly under conditions of low electron flux (Lowe & Thorneley, 1984*a*). Thus the inactivation may not be an artefact of the protein-isolation procedure but a regulatory mechanism similar to that identified in *Rhodospirillum rubrum* (Lowery & Ludden, 1985) and other nitrogen-fixing bacteria (Saari *et al.*, 1986, and references therein).

In the present paper we have used indigocarmine-oxidized Kp2 with a similar specific activity to that used by Lowe & Thorneley (1984*a*,*b*). The ability of the active and inactive forms of this protein to undergo reduction by $SO_2^{-\cdot}$, to bind MgADP and to undergo a conformation change has been investigated. The stoichiometry and kinetics of MgADP binding to $Kp2_{ox}$ have been determined, and the rates of interconversion of the two conformers of $Kp2_{ox}$ that exhibit different reactivity with respect to the reductant $SO_2^{-\cdot}$ have been estimated. The results also provide further insight into the pathway by which $Kp2_{ox}(MgADP)_2$ is converted into $Kp2(MgATP)_2$ in the catalytic cycle of nitrogenase action. The stoichiometry of $Kp2(MgATP)_2$ binding to Kp1 has also been reinvestigated and the results analysed in terms of the proportion of active Kp2 and the Mo content of the Kp1.

MATERIALS AND METHODS

Enzyme preparation

The nitrogenase component proteins from *Klebsiella pneumoniae* (*oxytoca*) N.C.I.B. 12204 were purified, assayed and the Mo and Fe contents determined as previously described (Thorneley & Lowe, 1983). Kp1 protein had a specific activity of 1800 nmol of ethylene produced·min^{-1}·mg of $protein^{-1}$ contained 1.30 ± 0.1 g-atom of Mo·mol^{-1}. Kp2 protein had a specific activity of 1500 nmol of ethylene produced·min^{-1}·mg of $protein^{-1}$ and contained 3.7 ± 0.2 g-atom Fe·mol^{-1}. The e.p.r. signal with $g_{av.} = 1.95$ integrated to 0.5 electron spins/mol of Kp2.

Kp2 protein was oxidized with indigocarmine dye (AnalaR grade; BDH Chemicals, Poole, Dorset, U.K.), which had been immobilized on an anion-exchange resin (Dowex AG1-X8; Bio-Rad, Watford, Herts., U.K.). Pre-washed resin was equilibrated with an aqueous saturated solution of indigocarmine, and excess dye was removed by washing on a sintered-glass funnel with distilled water. The dark-blue-coloured redox-active resin was suspended in deoxygenated buffer (25 mM-Hepes/10 mM-$MgCl_2$, pH 7.4) and used as follows. A column was set up comprising, sequentially from its base, Bio-Gel P-6DG (Bio-Rad) (20 cm × 0.7 cm), native washed Dowex AG1-X8 resin (1.0 cm × 0.7 cm) and Dowex AG1-X8 with bound indigocarmine (5.0 cm × 0.7 cm). The small layer of native Dowex AG1-X8 resin binds any dye displaced from the redox-active resin during downward elution of the protein. The Bio-Gel P-6DG also removes oxidation products and ensures that the eluted oxidized Kp2 protein is in a defined buffer. After equilibration of the column with deoxygenated buffer (25 mM-Hepes/10 mM-$MgCl_2$, pH 7.4), Kp2 protein (1 ml; 30 mg/ml with 1 mM-$Na_2S_2O_4$) was loaded on to the column and kept in contact with the redox-active resin for about 20 min. The top 0.2 cm of the redox-active resin turned orange, presumably owing to the rapid reaction with $Na_2S_2O_4$, but the large excess of bound dye equivalents ensured that the bulk of the resin did not change colour. Oxidized Kp2 protein (~ 1.5 ml) was eluted from the column, and the degree of oxidation (85–97%) was determined by e.p.r. spectroscopy using the amplitude of the feature at $g = 1.95$ relative to that of a sample of protein which had been reduced by $Na_2S_2O_4$ (1 mM). Oxidized Kp2 protein samples had specific activities in the range 1450–1750 nmol of

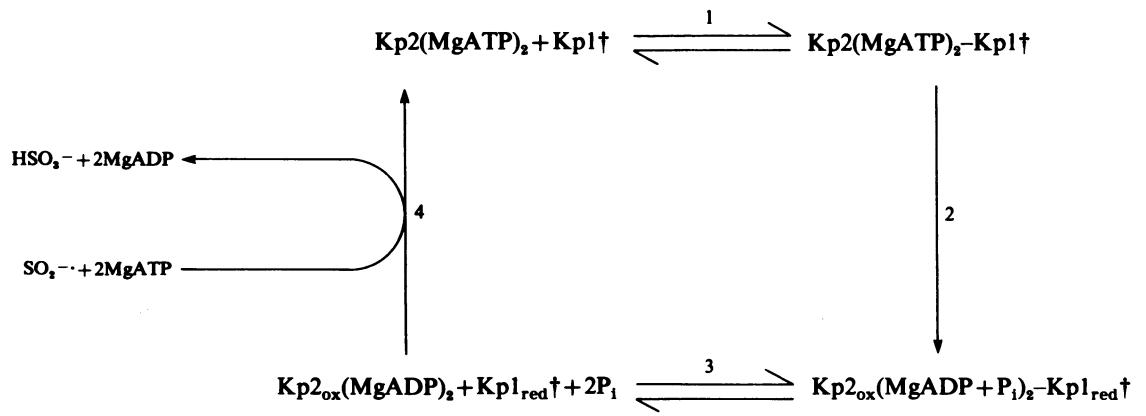

Scheme 1. Oxidation–reduction cycle for the Fe protein

Kp1† represents one of two independently functioning halves of the tetrameric ($\alpha_2\beta_2$ structure) Kp1. Each Kp1† is assumed to contain one Mo substrate-binding site and one Kp2-binding site. $SO_2^{-\cdot}$ in the active reductant formed by the predissociation of dithionite ion ($S_2O_4^{2-} \rightleftharpoons 2SO_2^{-\cdot}$).

ethylene produced $min^{-1} \cdot mg$ of $protein^{-1}$, which indicated either no loss of, or a marginal increase in, specific activity relative to that of the native protein. No Fe was lost during the oxidation procedure.

All biochemicals were purchased from Sigma Chemical Co., Poole, Dorset, U.K., and salts from BDH Chemicals, Poole, Dorset, U.K. Sodium dithionite (80–85% purity) solutions were standardized by spectrophotometric titration with K_3FeCN_6. All reactions were studied in a medium containing 25 mM-Hepes buffer (pH 7.4)/10 mM-$MgCl_2$ at 23 °C.

Instrumentation

Stopped-flow spectrophotometry was performed with a commercially available Aminco apparatus (0.92 cm pathlength) modified to improve thermostatic control (Thorneley, 1974). The apparatus was installed in a high-integrity glove box through which N_2 gas was circulated and an O_2 concentration less than 1 p.p.m. maintained (Thorneley & Lowe, 1983). Protein and reagent solutions were prepared inside the glove box. Oxidized Kp2 protein in both the presence and absence of MgADP retained full activity over the periods of up to 4 h that were necessary to complete kinetic experiments. Kp2 samples for e.p.r. spectroscopy were prepared in the glove box as previously described (Thorneley & Lowe, 1983) and spectra recorded on a Bruker ER200D e.p.r. spectrometer at 18 K, 20 mW power at 9.4 GHz, using 10 G field modulation at 100 kHz. U.v.–visible absorption spectra were recorded on a Perkin–Elmer Lambda-5 spectrophotometer, thermostatically controlled at 23 °C in quartz cuvettes (1 cm pathlength).

Stopped-flow data were recorded and analysed on a Digital Equipment Co. PDP1134A computer interfaced to the stopped-flow spectrophotometer via a BBC model B microcomputer. Rate constants were obtained by fitting the recorded data to exponential functions using least-squares minimization and NAG subroutine E04JBF.

Kinetic theory

The dissociation reaction of dithionite ion ($S_2O_4^{2-}$) (eqn. 1) complicates the kinetic analysis of reactions in which it acts as a reductant (eqn. 2) (A is the species being reduced to give the product, B):

$$S_2O_4^{2-} \underset{k_{-1}}{\overset{k_{+1}}{\rightleftharpoons}} 2SO_2^{-\cdot} \quad (1)$$

$$SO_2^{-\cdot} + A \xrightarrow{k_{+2}} SO_2 + B \quad (2)$$

Although both $S_2O_4^{2-}$ and $SO_2^{-\cdot}$ have been shown to be active species in the reduction of proteins (Lambeth & Palmer, 1973; Creutz & Sutin, 1973), only $SO_2^{-\cdot}$ functions in the nitrogenase system (Thorneley *et al.*, 1976, 1979; Watt & Burns, 1977; Hageman & Burris, 1978; Thorneley & Lowe, 1983).

Thorneley *et al.* (1976) showed that, for reactions of the type shown in eqn. (2), two rate expressions can be derived for two limiting cases. If $2k_{-1}[SO_2^{-\cdot}] \gg k_{+2}[A]$, then eqn. (3) is valid:

$$d[A]/dt = K_1^{\frac{1}{2}} k_{+2}[S_2O_4^{2-}]^{\frac{1}{2}} [A] \quad (3)$$

where $K_1 = k_{+1}/k_{-1} = 1.4$ nM at 23 °C (Thorneley & Lowe, 1983).

This predicts an exponential absorption change associated with the disappearance of A with an observed first-order rate constant ($K_1^{\frac{1}{2}} k_{+2}$) that is a linear function of the square root of the dithionite-ion concentration. This rate expression applies to $Kp2_{ox}(MgADP)_2$ species with $[S_2O_4^{2-}] > 1$ mM.

The second limiting case is when $k_{+2}[A] \gg 2k_{-1}[SO_2^{-\cdot}]$; then eqn. (4) applies:

$$d[A]/dt = 2k_{+1}[S_2O_4^{2-}] \quad (4)$$

The reaction will be zero-order in [A], and linear absorbance changes associated with the disappearance of A will be observed. The slopes of these changes will be proportional to the dithionite-ion concentration. This rate expression applies to the reduction of $Kp2_{ox}$ in the absence of MgADP with $[S_2O_4^{2-}] < 300$ μM. However, towards the end of these reactions, as $[A] \rightarrow 0$, $k_{+2}[A]$ is no longer $\gg 2k_{-1}[SO_2^{-\cdot}]$, and the kinetics change to first-order in A (limiting case 1 above).

RESULTS AND DISCUSSION

Stoichiometry and kinetics of reduction of $Kp2_{ox}$ by $Na_2S_2O_4$

E.p.r. spectroscopy showed that the Kp2 was 87% oxidized, giving $Kp2_{ox}$ and Kp2 concentrations of 72 μM and 11 μM respectively. Fig. 1 shows a typical trace for the absorbance changes at 430 nm when this protein solution was mixed in the stopped-flow spectrophotometer with $Na_2S_2O_4$ (8–250 μM before mixing). The essentially linear time-course reduction indicates a reaction that is zero-order in $[Kp2_{ox}]$, i.e. eqn. (4) is the appropriate rate expression. This is confirmed by the data in Fig. 2, which show a linear dependence, through the origin of the initial slopes of the absorbance–time traces on the concentration of $S_2O_4^{2-}$ in the range 40–250 μM after mixing. The gradient of the line in Fig. 2 corresponds to 16.2×10^3 absorbance units $s^{-1} \cdot M^{-1}$. Eqn. (4) together with $k_{+1} = 1.8\ s^{-1}$ (Thorneley *et al.*, 1976) gives 4.5 $mM^{-1} \cdot cm^{-1}$ as the change in extinction coefficient ($\Delta\epsilon$) of $Kp2_{ox}$ at 430 nm on reduction. The absorbance change ($\Delta A = 0.18 \pm 0.01$) with $[S_2O_4] > 40$ μM was independent of $[S_2O_4^{2-}]$ and can be used with $\Delta\epsilon = 4.5\ mM^{-1} \cdot cm^{-1}$ to calculate the concentration of $Kp2_{ox}$ undergoing a rapid one-electron (see below) reduction. The calculated value of 43 μM compares with 36 μM determined directly by Folin–Ciocalteu estimation and e.p.r. spectroscopy.

A third independent method of determining the concentration of $Kp2_{ox}$ undergoing one-electron reduction is by a stopped-flow amplitude titration with $[S_2O_4^{2-}]$ varied over the range 4–250 μM. Fig. 3 shows the results of a titration with $[Kp2_{ox}] = 36$ μM. A sharp 'end point' occurs at $[S_2O_4^{2-}] = 16.5$ μM, i.e. 33 μM electron equivalents. This is exactly the concentration of redox-active $Kp2_{ox}$ that is calculated for a total concentration of 36 μM if it is assumed that the 3.7 g-atoms of Fe/mol of Kp2 are present only as 4Fe–4S clusters [i.e. $(36 \times 3.7)/4 = 33$ μM].

The one-electron reduction of $Kp2_{ox}$ by $SO_2^{-\cdot}$ must occur with a rate constant $10^9 > k_{+3} > 10^8\ M^{-1} \cdot s^{-1}$ for zero-order kinetics to be observed with

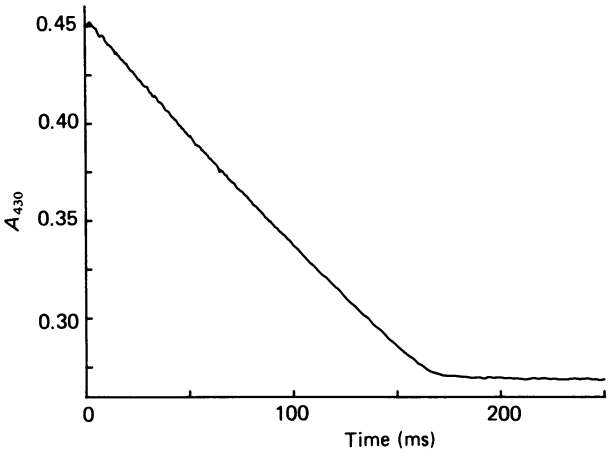

Fig. 1. Reduction of $Kp2_{ox}$ by $Na_2S_2O_4$ at 23 °C and at pH 7.4

$Kp2_{ox}$ was prepared as described in the text and the trace obtained by stopped-flow spectrophotometry at 430 nm as described in the Materials and methods section. The essentially linear absorbance–time curve is characteristic of a reaction that is zero-order in $[Kp2_{ox}]$, owing to rate-limiting dissociation of $S_2O_4^{2-}$ to give the active reductant $SO_2^{-\cdot}$. Syringe A: $[Kp2_{ox}] = 72\ \mu M$, $[Kp2] = 11\ \mu M$; syringe B: $[Na_2S_2O_4] = 164\ \mu M$. Both syringes contained Hepes (25 mM) and $MgCl_2$ (10 mM).

$[S_2O_4^{2-}] = 250\ \mu M$, assuming $K_1 = 1.4$ nM and a diffusion-controlled upper limit (Thorneley & Lowe, 1983). No correction has been made to the amplitudes for the reaction of predissociated $SO_2^{-\cdot}$ ($[SO_2^{-\cdot}] < 1\ \mu M$ when $[S_2O_4^{2-}] < 250\ \mu M$) with $Kp2_{ox}$ (36 μM) which must occur within the mixing time of the stopped-flow apparatus.

The observations and conclusions are essentially the same as those made previously for the initial phase of the reaction of $SO_2^{-\cdot}$ with $Ac2_{ox}$ (Thorneley *et al.*, 1976). However, with $Ac2_{ox}$, three subsequent slow phases were observed whose combined amplitudes were about the same as that of the rapid phase. $Kp2_{ox}$ exhibited much smaller slow phases whose combined amplitudes were less than 10% of that for the rapid phase. These have not been investigated because of the difficulties associated with looking at small absorbance changes over relatively long times with a single-beam stopped-flow spectrophotometer.

Reduction of $Kp2_{ox}$ by $Na_2S_2O_4$ in the presence of MgADP

Stopped-flow experiments were designed to investigate the stoichiometry and kinetics of MgADP binding to $Kp2_{ox}$ and the rate of the subsequent conformation change that yields the species designated as $Kp2^*_{ox}$-$(MgADP)_2$ in Scheme 2. The rate constants describing Scheme 2 are given in Table 1. The strategy employed relied upon the observation that $Kp2_{ox}$ and $Kp2^*_{ox}(MgADP)_2$ react at different rates with $SO_2^{-\cdot}$. The order of addition of $Kp2_{ox}$, MgADP and $Na_2S_2O_4$ and their relative concentrations in the two-syringe stopped-flow spectrophotometer enabled the competition between direct reduction of $Kp2_{ox}$ by $SO_2^{-\cdot}$ and the binding of MgADP to $Kp2_{ox}$, and the kinetics of a protein conformation change, to be studied.

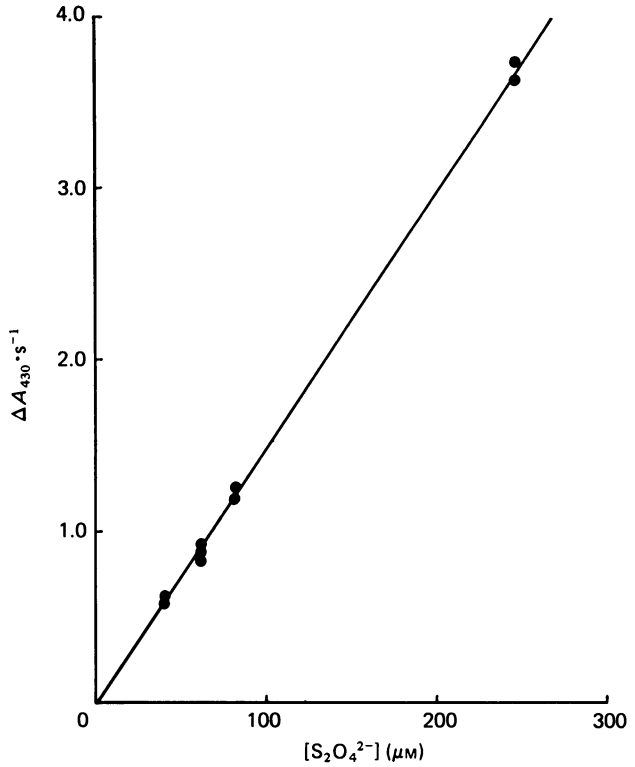

Fig. 2. Reduction of $Kp2_{ox}$ by $Na_2S_2O_4$ showing first-order dependence on $[Na_2S_2O_4]$ at 23 °C and at pH 7.4.

The initial slopes of stopped-flow absorbance–time traces (example shown in Fig. 1) are plotted as a function of initial $[Na_2S_2O_4]$. The linear dependence through the origin confirms that, under these conditions, the reaction is first-order in $[S_2O_4^{2-}]$, i.e. eqn. (4) is appropriate. Protein concentrations and reaction conditions were as for Fig. 1, with $[Na_2S_2O_4]$ varied from 80 to 500 μM in syringe B.

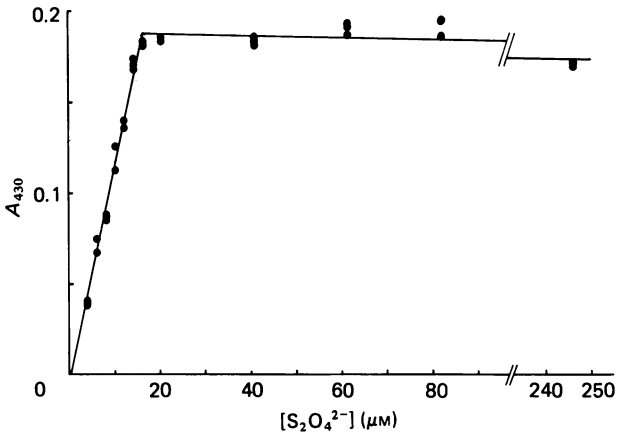

Fig. 3. Reduction of $Kp2_{ox}$ by $Na_2S_2O_4$ at 23 °C and at pH 7.4: stopped-flow amplitude titration

The amplitudes of traces such as that shown in Fig. 1 are plotted as a function of $[Na_2S_2O_4]$. The amplitude increases linearly up to $[Na_2S_2O_4] = 16.5\ \mu M$, after which it remains essentially constant, i.e. 33 μM electron equivalents were required to titrate $[Kp2_{ox}] = 36\ \mu M$. The protein concentrations and reaction conditions were as in Fig. 1, with $[Na_2S_2O_4]$ varied from 8 to 500 μM in syringe B.

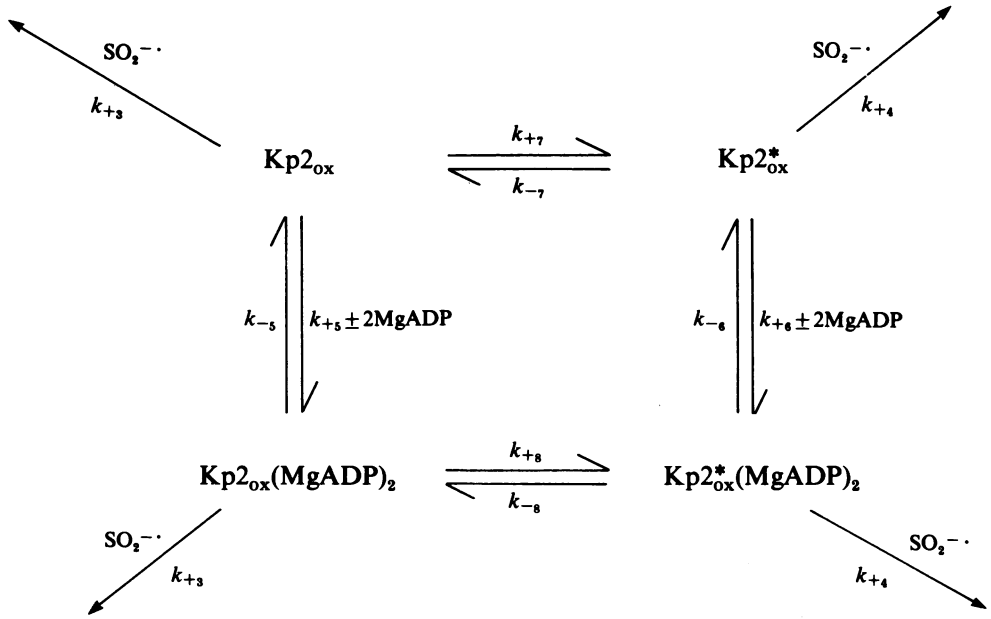

Scheme 2. Co-operative binding of two equivalents of MgADP to $Kp2_{ox}$ and reduction by $SO_2^{-\cdot}$ formed by the predissociation of dithionite ion

$Kp2_{ox}$ and $Kp2^*_{ox}$ represent two conformations of the oxidised Fe protein component from *K. pneumoniae* nitrogenase which are reduced by $SO_2^{-\cdot}$ at different rates (k_{+3} and k_{+4} respectively). K_5 and K_6 are composite equilibrium constants for the binding of two molecules of MgADP and are the products of the individual constants for the two successive binding processes. K_7 and K_8 are equilibrium constants for the conformation change in the free and MgADP-bound forms of the protein. The rate constants k_{+5} and k_{+6} refer to the binding of the first MgADP to $Kp2_{ox}$ and $Kp2^*_{ox}$ respectively. The rate constants k_{-5} and k_{-6} refer to the dissociation of the first MgADP from $Kp2_{ox}(MgADP)_2$ and $Kp2^*_{ox}(MgADP)_2$ respectively. These assumptions are based on the simplest model that explains the high degree of co-operativity for the binding of 2MgADP. The values for the rate constants are given in Table 1.

Table 1. Rate and equilibrium constants for the reactions shown in Scheme 2 and eqn. (1)

Sources of values were as follows: *, from Thorneley & Lowe (1983); †, the present work.

Rate or equilibrium constant	Value	Source
k_1	$1.7\ s^{-1}$	*
k_{-1}	$1.2\times10^9\ M^{-1}\cdot s^{-1}$	*
k_{+3}	$>10^8$, $<10^9\ M^{-1}\cdot s^{-1}$	†
k_{+4}	$3.0\times10^6\ M^{-1}\cdot s^{-1}$	*†
k_{+5}	$>3\times10^5$, $<3\times10^6\ M^{-1}\cdot s^{-1}$	†
k_{-5}	–	
k_{+6}	$>6\times10^6\ M^{-1}\cdot s^{-1}$	†
k_{-6}	$<2\ s^{-1}$	†
k_{+7}	$>6\times10^2$, $<6\times10^3 s^{-1}$	†
k_{-7}	$>1.2\times10^3$, $<1.2\times10^4\ s^{-1}$	†
k_{+8}	$>6\times10^2$, $<6\times10^3\ s^{-1}$	†
k_{-8}	$<2\ s^{-1}$	†
K_5K_8	$>4\times10^{10}\ M^{-2}$	†
K_6K_7	$>4\times10^{10}\ M^{-2}$	†
K_8	>300	†
K_7	$<5\times10^{-2}$	†

Stoichiometry and equilibrium constants for MgADP binding

Fig. 4 shows stopped-flow traces obtained for the reduction of $Kp2_{ox}$ by $SO_2^{-\cdot}$ under three different initial conditions. Trace a is the absorbance after mixing $Kp2_{ox}$ (45 μM) with buffer. Trace b shows the effect of pre-equilibrating $Kp2_{ox}$ (45 μM) with MgADP (250 μM) before mixing with $Na_2S_2O_4$ (16 mM) and MgADP (250 μM) in the stopped-flow apparatus. The curve is a single-exponential function ($k_{obs.} = 12.5\ s^{-1}$) with an amplitude corresponding to $\Delta\epsilon_{430} = 4.0\ mM^{-1}\cdot cm^{-1}$ (based on total $Kp2_{ox}$ concentration). Under these conditions the reaction of $Kp2_{ox}(MgADP)_2$ with $SO_2^{-\cdot}$ can be monitored and eqn. (3) used to calculate k_{+4} ($= 3.0\times10^6\ M^{-1}\cdot s^{-1}$) (see also Fig. 8 below). Trace c was obtained when $Kp2_{ox}$ (45 μM), pre-equilibrated with MgADP (30 μM), was mixed with $Na_2S_2O_4$ (16 mM) and MgADP (30 μM). The rapid initial absorbance change (complete within the mixing time) is attributable to the reaction of free $Kp2_{ox}$ (66% of the total protein) with $SO_2^{-\cdot}$ ($k_{+3} > 10^8\ M^{-1}\cdot s^{-1}$). The single exponential decay ($k_{obs.} = 12.5\ s^{-1}$), with a decreased amplitude relative to trace b, is due to the reaction of the 34% of the protein present as $Kp2_{ox}(MgADP)_2$ with $SO_2^{-\cdot}$ ($k_{+4} = 3.0\times10^6\ M^{-1}\cdot s^{-1}$). Trace d was obtained when $Kp2_{ox}$ (45 μM) was mixed with $Na_2S_2O_4$ (16 mM) in the absence of MgADP. The whole reaction was complete within the mixing time ($k_{+3} > 10^8\ M^{-1}\cdot s^{-1}$).

Fig. 5 shows amplitudes of curves similar to traces b and c in Fig. 4 as a function of the concentration of MgADP, which was pre-equilibrated with $Kp2_{ox}$ in one syringe of the stopped-flow apparatus. The relative concentrations of $Kp2_{ox}$ and $Kp2_{ox}(MgADP)_2$ are determined by these initial conditions. The same concentration of MgADP was also included with $Na_2S_2O_4$ (16 mM) in the other syringe in order to

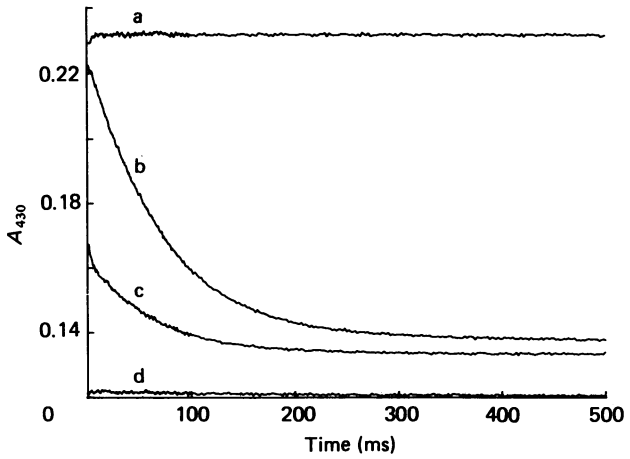

Fig. 4. Comparison of the rates of reduction of $Kp2_{ox}$ and $Kp2_{ox}(MgADP)_2$ by $Na_2S_2O_4$ at 23 °C and at pH 7.4

$Kp2_{ox}$ (45 μM) with Kp2 (< 2 μM) was prepared as described in the text and traces obtained by stopped-flow spectrophotometry at 430 nm as described in the Materials and methods section. Trace a: syringe A contained $[Kp2_{ox}] = 45$ μM; syringe B contained buffer. Trace b: syringe A contained $Kp2_{ox}$ (45 μM) and MgADP (250 μM); syringe B contained MgADP (250 μM) and $Na_2S_2O_4$ (16 mM). The curve is a single exponential function with $k_{obs.} = 12.5\ s^{-1}$, $\Delta\epsilon_{430} = 4.0\ mM^{-1}\cdot cm^{-1}$ on the basis of the total $Kp2_{ox}$ concentration. Trace c: syringe A contained $Kp2_{ox}$ (45 μM) and MgADP (30 μM); syringe B contained MgADP (30 μM) and $Na_2S_2O_4$ (16 mM). The curve is a single exponential function with $k_{obs.} = 12.5\ s^{-1}$ and an amplitude ~ 33% of that of trace b. Trace d: syringe A contained $[Kp2_{ox}] = 45$ μM; syringe B contained $Na_2S_2O_4$ (16 mM). Both syringes in all experiments in addition contained Hepes (25 mM) and $MgCl_2$ (10 mM).

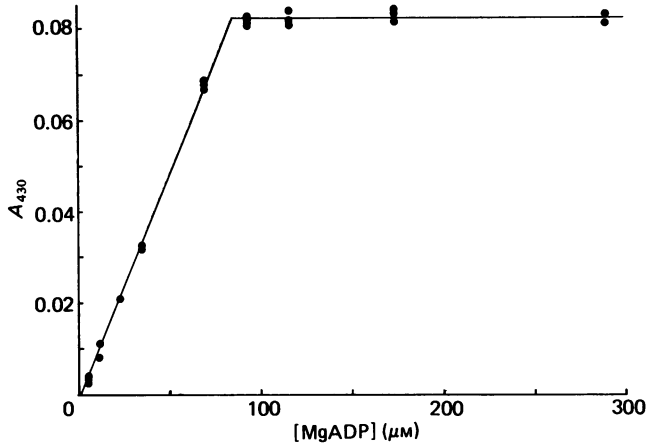

Fig. 5. Stoichiometry of MgADP binding to $Kp2_{ox}$ at 23 °C and at pH 7.4

The amplitudes of stopped-flow traces similar to those shown in Fig. 4 (traces b and c) are plotted as a function of [MgADP] (6–290 μM) preincubated with $Kp2_{ox}$ (45 μM), Kp2 (< 2 μM) in syringe A. Syringe B contained the same concentrations of MgADP and in every case the $Na_2S_2O_4$ concentration was 16 mM. The stoichiometry of MgADP binding at the 'break point' in the graph, [MgADP] = 87 μM with $[Kp2_{ox}] = 45$ μM, is 1.9:1. Because of the kinetics of the system, it is incorrect to use the mixed concentrations ([MgADP] = 87 μM; $[Kp2_{ox}] = 22.5$ μM), which would yield an $[MgADP]/[Kp2_{ox}]$ stoichiometry of 3.8:1 (see the text for an explanation).

suppress dissociation of bound MgADP from $Kp2_{ox}$ consequent on the 2-fold dilution occurring in the stopped-flow apparatus on mixing. However, only the MgADP in the syringe with the $Kp2_{ox}$ need be considered in the construction of Fig. 5. This is because free $Kp2_{ox}$, when mixed with solutions containing $Na_2S_2O_4$ (16 mM) and MgADP (< 250 μM) is reduced by $SO_2^{-\cdot}$ ($k_{+3} > 10^8\ M^{-1}\cdot s^{-1}$) before a significant amount of MgADP can bind ($k \sim 10^4\ M^{-1}\cdot s^{-1}$; see below and Fig. 6). The titration shows a linear increase in amplitude up to a molar ratio of MgADP to $Kp2_{ox}$ of 1.9(±0.1):1, after which the amplitude remains constant. A similar titration with $Kp2_{ox}$ (23 μM, before mixing) gave a molar ratio of MgADP to $Kp2_{ox}$ of 2.2(±0.2):1. In both titrations the maximum amplitude corresponded to a $\Delta\epsilon_{430}$ of 4.0±0.2 $mM^{-1}\cdot cm^{-1}$, based on the total $Kp2_{ox}$ concentrations. The kinetics of the observable change were independent of the MgADP concentration over the range 5–250 μM, with $k_{obs.} = 12\pm1\ s^{-1}$ at an $Na_2S_2O_4$ concentration of 16 mM ($k_{+4} = 3.0\times10^6\ M^{-1}\cdot s^{-1}$; see Fig. 8 below).

These data show that $Kp2_{ox}$ binds two equivalents of MgADP with a high degree of co-operativity. The linear decrease in amplitude, with data points down to [MgADP] = 6 μM, allows an estimate of the overall equilibrium constant K_7K_6 or $K_5K_8 > 4\times10^{10}\ M^{-2}$. A more detailed analysis of Scheme 2 can be made by assuming that $Kp2_{ox}$ and $Kp2_{ox}(MgADP)_2$ react with $SO_2^{-\cdot}$ at similar rates ($k_{+3} > 10^8\ M^{-1}\cdot s^{-1}$) and that $Kp2^*_{ox}$ and $Kp2^*_{ox}(MgADP)_2$ react at the same rate ($k_{+4} = 3\times10^6\ M^{-1}\cdot s^{-1}$), implying that the conformation change, not the binding of MgADP *per se*, causes a decrease in the rate of reduction by $SO_2^{-\cdot}$. This is reasonable, since electron-transfer rates can depend critically on the redox potentials of the reactants and it is known that both MgATP and MgADP decrease the midpoint potentials of nitrogenase Fe proteins by about 100 mV (Zumft *et al.*, 1974; Watt, 1985; Morgan *et al.*, 1986), a decrease accompanied by change in the e.p.r. spectrum of the reduced Fe proteins assignable to a protein conformation change which affects the 4Fe–4S cluster. No absorbance change occurs at 430 nm when MgADP binds to either oxidized or reduced Kp2 protein. The equilibrium between $Kp2_{ox}(MgADP)_2$ and $Kp2^*_{ox}(MgADP)_2$ must favour $Kp2^*_{ox}(MgADP)_2$ ($K_8 > 10$), since the initial absorbance of trace b, Fig. 4, is very close to that of trace a. If a significant concentration of $Kp2_{ox}(MgADP)_2$ were present at equilibrium with saturating MgADP, a rapid phase would have preceded the observed reaction progress curve and trace b would have had a decreased amplitude. Similarly, in the absence of MgADP, the equilibrium between $Kp2_{ox}$ and $Kp2^*_{ox}$ must favour $Kp2_{ox}$ ($K_7 < 5\times10^{-2}$), since no slow phase was detected on reduction by $SO_2^{-\cdot}$ (trace d, Fig. 4) (see also Fig. 7 and related discussion).

The absorbance changes for the reduction of $Kp2_{ox}$ in the absence of MgADP corresponded to an $\Delta\epsilon_{430}$ of 5.0±0.5 $mM^{-1}\cdot cm^{-1}$ (see data in Figs. 1, 3 and

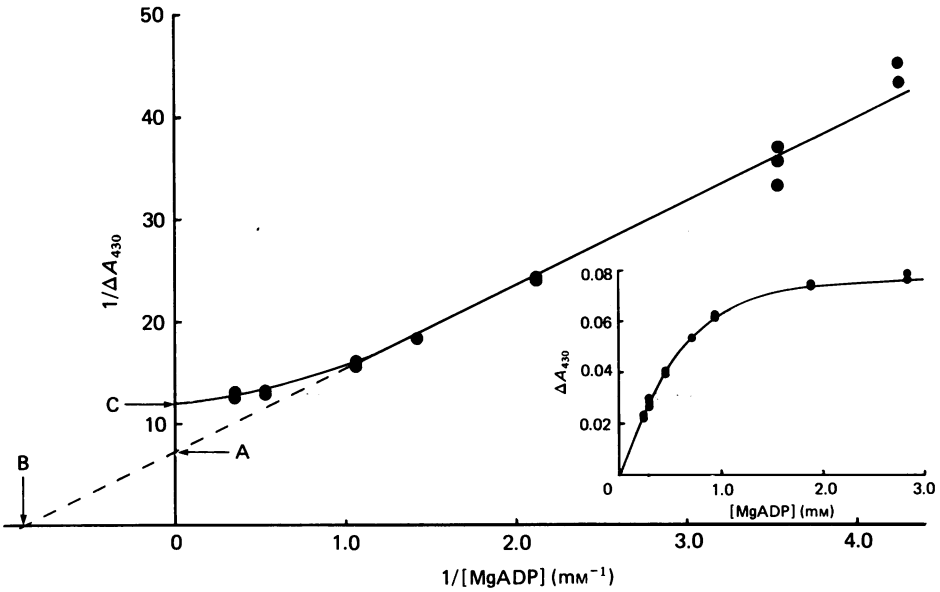

Fig. 6. Reduction of $Kp2_{ox}$ by $Na_2S_2O_4$ in the presence of MgADP: amplitude titration demonstrating comparable rates of reduction and protein conformation change at 23 °C and at pH 7.4

The inset shows the amplitudes of stopped-flow traces for the slow phase of reduction [$Kp2^*_{ox}(MgADP)_2$] by $SO_2^{-\cdot}$ as a function of [MgADP] at constant [$Na_2S_2O_4$] (8 mM). Syringe A contained $Kp2_{ox}$ (75 μM) and Kp2 (6 μM). Syringe B contained $Na_2S_2O_4$ (16 mM) and variable MgADP (0.5–5.6 mM). Both syringes contained Hepes (25 mM) and $MgCl_2$ (10 mM). The main Figure shows a double-reciprocal plot of the inset data. Point A was calculated using an $\Delta\epsilon_{430}$ value of 4.0 mM$^{-1}\cdot$cm^{-1}, with the assumption that all the $Kp2_{ox}$ was present as $Kp2^*_{ox}(MgADP)_2$.

4), whereas in the presence of MgADP, $\Delta\epsilon_{430} = 4.0 \pm 0.2$ mM$^{-1}\cdot$cm^{-1} (see Fig. 4). We consider this a real difference, but currently have no explanation.

Kinetics of MgADP binding to $Kp2_{ox}$ and of a subsequent conformation change

Scheme 2 shows that, if $Kp2_{ox}$ is not pre-equilibrated with MgADP, but exposed to $Na_2S_2O_4$ and MgADP simultaneously on mixing in the stopped-flow apparatus, then the ratio of the fast (k_{+3}) to the slow (k_{+4}) phases of reduction could depend on the relative concentrations of MgADP and $Na_2S_2O_4$. The data will be analysed initially assuming the dominant pathway involves k_{+5}, k_{-5}, k_{+8} and k_{-8}. The concentration ranges over which significant changes in amplitude will be observable are determined by the ratios k_{+3}/k_{+8} and k_{+4}/k_{-8}. We favour this pathway because of our failure to detect $Kp2^*_{ox}$ in equilibrium with $Kp2_{ox}$ in the absence of MgADP ($K_7 < 5 \times 10^{-2}$; see above). However, we cannot exclude the alternative pathway, k_{+7}, k_{-7}, k_{+6} and k_{-6}, and will comment on this subsequently.

The inset to Fig. 6 shows stopped-flow amplitude data for the slow phase [reduction of $Kp2^*_{ox}(MgADP)_2$ by $SO_2^{-\cdot}$] as a function of MgADP concentration. One syringe contained $Kp2_{ox}$ (62 μM) and the other $Na_2S_2O_4$ (16 mM) with [MgADP] varied from 0.5 to 5.6 mM. At low concentrations of MgADP, reduction of $Kp2_{ox}$ by $SO_2^{-\cdot}$ (k_{+3}) is the dominant pathway, and most of the reaction occurs within the mixing time (2 ms). As the concentration of MgADP increases, the binding of MgADP to $Kp2_{ox}$ (k_{+5}) and the consequent conformation change (k_{+8}) to yield $Kp2^*_{ox}(MgADP)_2$ compete effectively with the direct reduction of $Kp2_{ox}$ (k_{+3}). Fig. 6 shows a double-reciprocal plot for these data. The

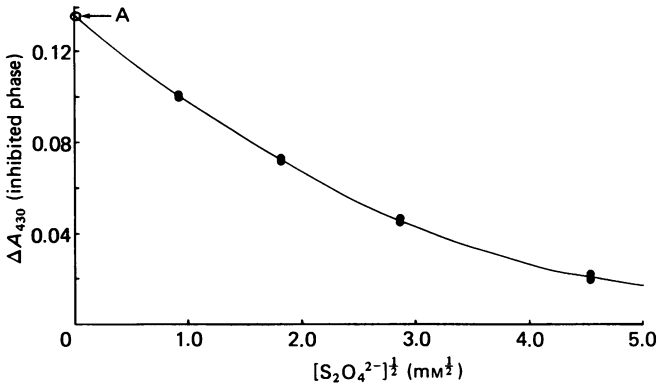

Fig. 7. Reduction of $Kp2_{ox}$ by $Na_2S_2O_4$ in the presence of MgADP: competition between reduction and binding of MgADP at 23 °C and at pH 7.4

The amplitude of the slow phase [reduction of $Kp2^*_{ox}(MgADP)_2$, k_{+4}] is plotted as a function of $[Na_2S_2O_4]^{\frac{1}{2}}$ at constant MgADP (0.5 mM after mixing). Syringe A contained $Kp2_{ox}$ (74 μM) and Kp2 (< 2 μM). Syringe B contained MgADP (1.0 mM) and $Na_2S_2O_4$ (0.8–40 mM); both syringes contained Hepes (25 mM) and $MgCl_2$ (10 mM). Point A was calculated by assuming complete conversion of $Kp2_{ox}$ into $Kp2^*_{ox}(MgADP)_2$ before reduction by $SO_2^{-\cdot}$, using an $\Delta\epsilon_{430}$ value of 4.0 mM$^{-1}\cdot$cm^{-1} and a 0.92 cm pathlength.

reciprocal amplitude (8.5) at infinite [MgADP], i.e. [MgADP]$^{-1} = 0$ (point A), was calculated by using a value of $\Delta\epsilon_{430}$ of 4.0 mM$^{-1}\cdot$cm^{-1} (see above and Fig. 5). The points in Fig. 6 at the five lowest MgADP concentrations fall on a straight line that extrapolates

through point A to give an abscissa intercept at [MgADP] = 1.0 mM (point B). At this concentration of MgADP, with $[S_2O_4^{2-}] = 8$ mM, half the $Kp2_{ox}$ is reduced directly (k_{+3}) and half after conversion into $Kp2^*_{ox}(MgADP)_2$ (k_{+4}). Under these conditions and assuming $k_{+8} \gg k_{+5}$ [MgADP] (see below), eqn. (5) applies:

$$k_{+3}[SO_2^{-\cdot}][Kp2_{ox}] = k_{+5}[MgADP][Kp2_{ox}] \quad (5)$$

Eqns. (1) and (5), together with $10^9 > k_{+3} > 10^8$ $M^{-1}\cdot s^{-1}$, give $3 \times 10^6 > k_{+5} > 3 \times 10^5$ $M^{-1}\cdot s^{-1}$. The linear amplitude-dependence in Fig. 6 at low MgADP concentrations and the high degree of co-operativity shown for the equilibrium binding of 2MgADP in Fig. 5 are consistent with the rapid binding of the second MgADP molecule relative to the first, i.e. k_{+5} is associated with the binding of the first MgADP.

At [MgADP] > 1 mM, the data points in Fig. 6 deviate from the straight line and extrapolate to a reciprocal amplitude of 12.5 (absorbance units)$^{-1}$ at [MgADP] = ∞ (point C). We explain these data as the reduction of the intermediate $Kp2_{ox}(MgADP)_2$ by $SO_2^{-\cdot}$ (k_{+3}) occurring at a rate comparable with that of the conformation change (k_{+8}) under these conditions ($[S_2O_4^{2-}] = 8$ mM). The difference between the observed (point C) and calculated (point A) amplitudes as [MgADP] $\rightarrow \infty$, represents the proportion of $Kp2_{ox}(MgADP)_2$ that reacts with $SO_2^{-\cdot}$ (k_{+3}) before it has undergone the conformation change to yield $Kp2^*_{ox}(MgADP)_2$ (k_{+8}). Eqn. (6) relates these amplitudes to the rate constants k_{+3} and k_{+8} as [MgADP] $\rightarrow \infty$.

$$\frac{k_{+3}[SO_2^{-\cdot}]}{k_{+8}} = \frac{\text{calculated} - \text{observed amplitude}}{\text{observed amplitude}} \quad (6)$$

$$= (0.12-0.08)/0.08 = 0.5 \text{ (data from Fig. 6)}$$

Since $10^8 < k_{+3} < 10^9$ $M^{-1}\cdot s^{-1}$, then with $[S_2O_4^{2-}] = 8$ mM, it follows that 3×10^3 $s^{-1} > k_{+3}$ $[SO_2^{-\cdot}] > 300$ s^{-1}. Eqns. (1) and (6) then yield 6×10^3 $s^{-1} > k_{+8} > 6 \times 10^2$ s^{-1}. The assumption above that at [MgADP] < 1 mM then $k_{+8} > k_{+5}$[MgADP] is validated provided it is remembered that the values of k_{+8} and k_{+5} both depend on the limit set for k_{+3} and therefore cannot be varied within their limits independently.

Fig. 7 shows the amplitude of the slow phase, [$Kp2^*_{ox}(MgADP)_2$ reacting with $SO_2^{-\cdot}$ via k_{+4}] as a function of $[S_2O_4^{2-}]^{\frac{1}{2}}$ at a constant MgADP concentration. One syringe contained $Kp2_{ox}$ and the other $Na_2S_2O_4$ and MgADP. As the concentration of $Na_2S_2O_4$ is increased, the amplitude of the slow phase decreases, owing to significant reduction of the rapidly reacting species $Kp2_{ox}$ and $Kp2_{ox}(MgADP)_2$ by $SO_2^{-\cdot}$ (k_{+3}) (Scheme 2). The point corresponding to $[Na_2S_2O_4] = 0$ was calculated by using an $\Delta\epsilon_{430}$ value of 4.0 $mM^{-1}\cdot cm^{-1}$, with the assumption that all the $Kp2_{ox}$ is present as the slow-reacting species $Kp2^*_{ox}(MgADP)_2$. The smooth extrapolation of the data points to the calculated point on the ordinate axis is consistent with our earlier conclusion that the equilibrium constant $K_8 = k_{+8}/k_{-8} > 10$ (see also Figs. 4 and 5 and related discussion). Similarly the conclusion that $K_7 < 5 \times 10^{-2}$ is consistent with the amplitude in Fig. 7 tending to zero as $[Na_2S_2O_4]$ increases.

Fig. 8 shows the observed first-order rate constants ($k_{obs.}$) for the slow phase as a function of $[S_2O_4^{2-}]^{\frac{1}{2}}$. These

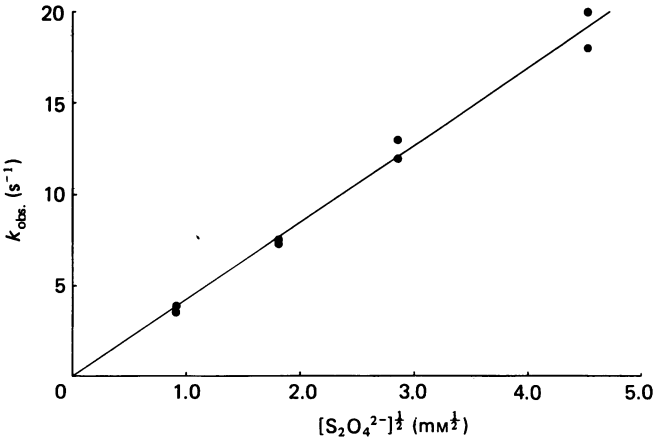

Fig. 8. Dependence of $k_{obs.}$ for the reduction of $Kp2^*_{ox}(MgADP)_2$ on $[Na_2S_2O_4]^{\frac{1}{2}}$ at 23 °C and at pH 7.4

The observed first-order rate constant ($k_{obs.}$) for the slow phase of reduction of $Kp2_{ox}$ in the presence of MgADP is shown as a function of $[Na_2S_2O_4]^{\frac{1}{2}}$. The corresponding amplitude-dependence is shown in Fig. 7, together with the experimental details. The slope and eqn. (3) give $k_{+4} = 3.0 \times 10^6$ $M^{-1}\cdot s^{-1}$ for the reduction of $Kp2^*_{ox}(MgADP)_2$ by $SO_2^{-\cdot}$.

data are from the same experiments that yielded the amplitudes shown in Fig. 7. The linear dependence through the origin confirms a reaction with $SO_2^{-\cdot}$ as the active reductant and, using eqn. 3 (with k_{+4} replacing k_{+2}), the slope yields $k_{+4} = 3.0 \times 10^6$ $M^{-1}\cdot s^{-1}$, in agreement with a previously obtained value (Thorneley & Lowe, 1983). At the lowest concentration of $Na_2S_2O_4$ (0.8 mM), $k_{obs.} = 3.7$ s^{-1}, and this allows an estimate of $k_{-8} < 2$ s^{-1} to be made. If k_{-8} were larger, then the line in Fig. 8 would curve towards a limiting value of $k_{obs.} > 0$ as $[Na_2S_2O_4] \rightarrow 0$. If $k_{-8} < 2$ s^{-1}, and with 6×10^3 $s^{-1} > k_{+8} > 6 \times 10^2$ s^{-1} (eqn. 6 and related discussions above) then $K_8 = k_{+8}/k_{-8} > 300$, which is consistent with the estimate of $K_8 > 10$ made above after consideration of trace b (Fig. 4).

The alternative pathway involving k_{+7}, k_{-7}, k_{+6} and k_{-6} in Scheme 2 will now be considered. The data in Fig. 6 show that when [MgADP] = 1 mM with $[Na_2S_2O_4] = 8$ mM (intercept B), half of the $Kp2_{ox}$ is reduced directly (k_{+3}) and half after conversion into $Kp2^*_{ox}$ or $Kp2^*_{ox}(MgADP)_2$ (k_{+4}). At these concentrations of MgADP and $Na_2S_2O_4$, eqn. (7) applies:

$$k_{+3}[SO_2^{-\cdot}] = K_7 k_{+6}[MgADP] \quad (7)$$

assuming $k_{-7} \gg k_{+6}$[MgADP]. Since $10^8 < k_{+3} < 10^9$ $M^{-1}\cdot s^{-1}$, then $3 \times 10^6 > K_7 k_{+6} > 3 \times 10^5$ $M^{-1}\cdot s^{-1}$, and with $K_7 < 5 \times 10^{-2}$, then $k_{+6} > 6 \times 10^6$ $M^{-1}\cdot s^{-1}$.

The curvature in Fig. 6 can be explained if, at [MgADP] > 1 mM, the conformation change (k_{+7}) limits the rate of conversion of $Kp2_{ox}$ into $Kp2^*_{ox}(MgADP)_2$. The ratio of the amplitudes calculated from the points A and C in Fig. 6 (ratio = 0.5; eqn. 6) are related to k_3 and k_7 by eqn. (8) and with $10^8 < k_{+3} < 10^9$ $M^{-1}\cdot s^{-1}$, at $[S_2O_4^{2-}] = 8$ mM, then:

$$k_{+3}[SO_2^{-\cdot}]/k_{+7} = 0.5 \quad (8)$$

6×10^3 $s^{-1} > k_{+7} > 6 \times 10^2$ s^{-1}. Using the upper limit for $K_7 < 5 \times 10^{-2}$, it follows that $k_{-7} > 1.2 \times 10^4$ s^{-1}.

The linear dependence of the data in Fig. 8 imposed a

limit for $k_{-6} < 2\ s^{-1}$. If k_{-6} were larger than this, then Fig. 8 would show a non-linear dependence on $[S_2O_4^{2-}]^{\frac{1}{2}}$, with curvature towards a positive intercept ($k_{obs.} > 0$ as $[S_2O_4^{2-}]^{\frac{1}{2}} \rightarrow 0$). This would occur because, with $k_{-7} > 1.2 \times 10^4\ s^{-1}$ and at $[S_2O_4^{2-}] = 0.8$ mM, the reduction of $Kp2_{ox}$ (k_{+3}) is relatively fast, i.e. the slow dissociation of MgADP prevents the reduction of $Kp2^*_{ox}(MgADP)_2$ occurring by conversion into $Kp2_{ox}$ via k_{-6} and k_{-7}. We assign k_{-6} to the dissociation of the first MgADP from $Kp2^*_{ox}(MgADP)_2$, and k_{+6} to the association of the first MgADP to $Kp2^*_{ox}$, only because of the high co-operativity exhibited by $Kp2_{ox}$ in binding 2MgADP (Fig. 5). The data do not allow a more complete analysis in which the sequential binding and dissociation of 2MgADP are considered.

Hammes & Hurst (1969) measured the rate constants for MgADP binding ($k = 5 \times 10^6\ M^{-1} \cdot s^{-1}$) and a subsequent induced conformation change ($1.7 \times 10^4\ s^{-1}$) in creatine kinase (EC 2.7.3.2.) at 11 °C by using temperature-jump relaxation methods. These values are similar to those determined above for the analogous reactions occurring with $Kp2_{ox}$ ($3 \times 10^5 < k_{+5} < 3 \times 10^6\ M^{-1} \cdot s^{-1}$; $6 \times 10^2 < k_{+8} < 6 \times 10^3\ s^{-1}$). Thus the presence of a 4Fe–4S cluster, which is thought to undergo some distortion as a result of the protein conformation change (Lindahl *et al.*, 1985), does not greatly alter the kinetics of the conformation change. It is also consistent with the model of Hausinger & Howard (1983) for Av2, which shows MgADP binding at some distance from the 4Fe–4S cluster, which requires the effects of MgADP on the 4Fe–4S cluster to be mediated by the protein.

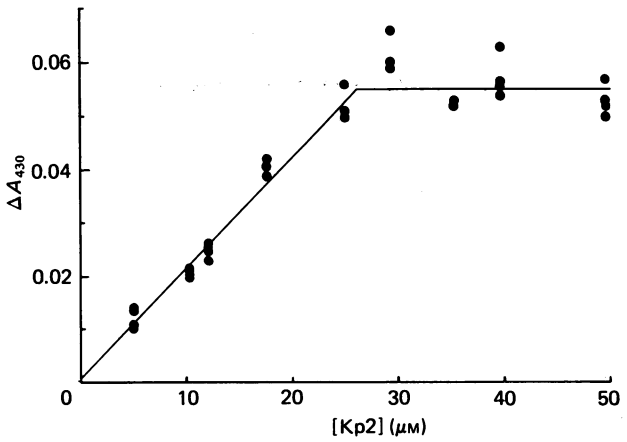

Fig. 9. Electron transfer from $Kp2(MgATP)_2$ to Kp1: stopped-flow amplitude titration to determine the competence of Kp2 to effect this reaction

The electron transfer from $Kp2(MgATP)_2$ to Kp1 was monitored at 430 nm. The amplitude of the single-exponential absorbance change associated with the oxidation of $Kp2(MgATP)_2$ to yield $Kp2_{ox}(MgADP + P_i)_2$ is plotted as a function of $[Kp2(MgATP)_2]$ at a fixed [Kp1]. Syringe A contained Kp1 (19 μM), Kp2 (10–100 μM) and $Na_2S_2O_4$ (1.0 mM). Syringe B contained ATP (18 mM) and $Na_2S_2O_4$ (1.0 mM). Both syringes contained Hepes (25 mM) and $MgCl_2$ (10 mM). The 'break point' occurs at a [Kp2]/[Mo] ratio of 2.25, consistent with the Kp2 sample being only 45% active with respect to its competence at Kp1 reduction.

Electron transfer from $Kp2(MgATP)_2$ to Kp1

$Kp2(MgATP)_2$ associates with Kp1 ($k > 5 \times 10^7\ M^{-1} \cdot s^{-1}$) and is oxidized in an electron-transfer reaction that it coupled with the hydrolysis of MgATP ($k = 2 \times 10^2\ s^{-1}$) (steps 1 and 2 in Scheme 1; see also Thorneley, 1975; Eady *et al.*, 1978; Thorneley & Lowe, 1983; Lowe & Thorneley, 1984*a*,*b*). The oxidation of $Kp2(MgATP)_2$ by Kp1 has been monitored in the stopped-flow spectrophotometer as a single exponential increase in absorbance at 430 nm ($\tau = \sim 8$ ms with [Kp1] = 9 μM, [Kp2] varied from 5 to 50 μM, [MgATP] = 9 mM, $[Na_2S_2O_4] = 1.0$ mM, pH 7.4, 23 °C). Under these conditions, the dissociation of the post-electron-transfer complex, $Kp2_{ox}(MgADP)_2$–$Kp1_{red}$, and subsequent reduction of $Kp2_{ox}(MgADP)_2$ by $SO_2^{-\cdot}$ are relatively slow (Thorneley & Lowe, 1983). Therefore the amplitude of the absorbance change for the electron transfer reaction (step 2, Scheme 1) can be used to determine the competence of $Kp2(MgATP)_2$ to effect the reduction of Kp1. Fig. 9 shows amplitude data for a titration of Kp1 (9 μM) with Kp2. The amplitude increases in a linear manner up to [Kp2] = 27 ± 2 μM, when it remains constant (0.06 absorbance units corrected to a 1 cm pathlength). Lowe & Thorneley (1984*a*) showed that the Mo content of Kp1 determined the number of active sites for electron transfer from $Kp2(MgATP)_2$. The Kp1 used in these studies contained 1.3 g-atom of Mo/mol of Kp1. Since 27 μM-$Kp2(MgATP)_2$ was required to saturate 12 μM Mo sites (Fig. 9), we conclude that the Kp2 was only 45% active with respect to electron transfer to Kp1. This conclusion is consistent with the ratio of the measured specific activity (1500 nmol of H_2 produced · min^{-1} · mg of $Kp2^{-1}$) to the maximum theoretical specific activity predicted by Thorneley & Lowe (1984*b*) of 4000 ± 800 nmol of H_2 produced · min^{-1} · mg of $Kp1^{-1}$. The single exponential increase in absorbance and the data in Fig. 9 are also consistent with the assumption of Lowe & Thorneley (1984*a*,*b*) and Thorneley & Lowe (1984*b*) that inactive $Kp2(MgATP)_2$ binds to Kp1 at least ten times more slowly ($k = 4 \times 10^6\ M^{-1} \cdot s^{-1}$) than does active $Kp2(MgATP)_2$ ($k > 5 \times 10^7\ M^{-1} \cdot s^{-1}$). Thus active $Kp2(MgATP)_2$ always competes effectively with inactive $Kp2(MgATP)_2$ for the binding sites on Kp1 before electron transfer.

The maximum amplitude of 0.06 absorbance units and the active-site concentration determined by the Mo content of the Kp1 (12 μM), gives a $\Delta\epsilon_{430}$ of $5\ mM^{-1} \cdot cm^{-1}$. The difference between this value and that for the reduction of dye oxidized $Kp2_{ox}(MgADP)_2$ ($4\ mM^{-1} \cdot cm^{-1}$) is most likely due to the small decrease in absorbance occurring for Kp1 on reduction.

Fig. 2 of Stephens *et al.* (1978) gives $\Delta\epsilon_{430} = 5.3\ mM^{-1} \cdot cm^{-1}$ for $Av2_{ox}(MgADP)_2$–Av2 (specific activity of 2000 ± 100 nmol of ethylene produced · min^{-1} · mg of $protein^{-1}$. Ljones & Burris (1978) measured $\Delta\epsilon_{430} = 3.77\ mM^{-1} \cdot cm^{-1}$ for $Cp2_{ox}$-$(MgADP)_2$–Cp2 (specific activity of 1700 nmol of $S_2O_4^{2-}$ oxidized min^{-1} · mg of $protein^{-1}$. However, they then corrected this value to $6.6\ mM^{-1} \cdot cm^{-1}$ by assuming that only 57% of the Cp2 had been oxidized. This was based on the ability of 57% of the Cp2 to undergo an MgATP-induced conformation change that labilizes the Fe to chelation by bathophenanthrolinedisulphonate. Our results show that Ljones & Burris (1978) were probably correct in using the bathophenanthroline/

MgATP assay as a measure of the percentage of Fe protein capable of transferring one electron to MoFe protein in a reaction induced by MgATP, but were not correct in adjusting the value of $\Delta\epsilon_{430}$. We suggest that, in their experiments, all the Cp2 was oxidized by Cp1 in the presence of MgATP after exhaustion of dithionite ion. However, only 57% of Cp2 was oxidized by direct electron transfer to Cp1. The remaining 43%, which was incapable of responding to MgATP, was oxidized indirectly by Cp1, with active $Cp2_{ox}$ and Cp2 acting as mediators, i.e. active and inactive Cp2 are in redox equilibrium. This is consistent with the complete 'bleaching' of the e.p.r. signal of reduced Cp2 in this type of experiment. We therefore conclude that $\Delta\epsilon_{430} = 4.5 \pm 0.8$ for the one-electron oxidation of the 4Fe–4S cluster in Kp2, Av2 and Cp2 proteins and that this value depends only on the Fe content and not on the specific activity. This value is significantly lower than 7.0 $mM^{-1} \cdot cm^{-1}$ (Stombaugh *et al.*, 1976) and 6.3 $mM^{-1} \cdot cm^{-1}$ (calculated from Fig. 6 of Stephens *et al.*, 1978) for 4Fe–4S clusters in various ferredoxins. The difference in electronic configuration that changes $\Delta\epsilon_{430}$ may be related to the $S = 3/2$ e.p.r. signal that is seen with reduced nitrogenase Fe proteins but not with ferredoxins.

Conclusions

Kp2, with a specific activity of 1500 nmol of H_2 produced $\cdot min^{-1} \cdot$ mg of $protein^{-1}$, is heterogeneous: only 45% of the protein is capable of effecting MgATP-dependent reduction of Kp1. However, the defect or modification that causes 55% of the protein to be inactive in electron transfer to Kp1 does not prevent $Kp2_{ox}$ undergoing a rapid single-electron reduction by $SO_2^{-\cdot}$ ($10^8\ M^{-1} \cdot s^{-1} < k_{+3} < 10^9\ M^{-1} \cdot s^{-1}$). This implies that all the protein molecules contain a single 4Fe–4S cluster that is redox-active. All the $Kp2_{ox}$ is capable of binding 2MgADP and undergoing a conformation change that causes $Kp2^*_{ox}(MgADP)_2$ to react much more slowly with $SO_2^{-\cdot}$ ($k_{+4} = 3.0 \times 10^6\ M^{-1} \cdot s^{-1}$). The binding of 2MgADP is highly co-operative, and only an upper limit for a composite association constant can be determined ($K_5K_8 > 4 \times 10^{10}\ M^{-2}$). MgADP binds to both $Kp2_{ox}$ ($3 \times 10^6 > k_{+5} > 3 \times 10^5\ M^{-1} \cdot s^{-1}$) and $Kp2^*_{ox}$ ($k_{+6} > 6 \times 10^6\ M^{-1} \cdot s^{-1}$) rapidly. Dissociation of MgADP from $Kp2^*_{ox}(MgADP)_2$ is too slow ($k_{-6} < 2\ s^{-1}$) to occur significantly in the catalytic cycle of nitrogenase. If the less-reactive form $Kp2^*_{ox}$ is present in equilibrium with $Kp2_{ox}$ in the absence of MgADP, it comprises less than 5% of the total protein ($K_7 < 5 \times 10^{-2}$). However, even at this concentration it could provide a pathway by which essentially all the $Kp2_{ox}$ can be converted into $Kp2^*_{ox}(MgADP)_2$ (k_{+7}, k_{+6}). However a more likely route involves an MgADP-induced conformation change (k_{+5}, k_{+8}) with $Kp2^*_{ox}(MgADP)_2$ stabilized relative to $Kp2(MgADP)_2$ ($K_8 > 300$). Both mechanisms have been considered, and it is not possible to distinguish between them with the present data. In both cases the less-reactive form, $Kp2^*_{ox}(MgADP)_2$, is constrained to react directly with $SO_2^{-\cdot}$ by either a low rate of dissociation of MgADP ($k_{-6} < 2\ s^{-1}$) or a low rate of conversion into the more reactive form, $Kp2(MgADP)_2$ ($k_{-8} < 2\ s^{-1}$). Thus, in the catalytic cycle of nitrogenase with $Na_2S_2O_4$ as reductant, reduction of $Kp2^*_{ox}(MgADP)_2$ must precede the exchange of MgATP for MgADP. The exchange reaction on reduced Kp2 has been shown to be rapid (limited by the release of MgADP with $k \sim 2 \times 10^2\ s^{-1}$; Thorneley & Cornish-Bowden, 1977).

We thank Mr. Karl Fisher for e.p.r. measurements, Professor M. J. Dilworth, Dr. R. Eady and Dr. D. J. Lowe for helpful discussion, and Professor J. R. Postgate for his comments on the manuscript.

REFERENCES

Burgess, B. K. (1985) in Molybdenum Enzymes (Spiro, T. G., ed.) (Metal Ions in Biology Series, vol. 7), pp. 161–219, Wiley–Interscience, New York

Creutz, C. & Sutin, N. (1973) Proc. Natl. Acad. Sci. U.S.A. **70**, 1701–1703

Eady, R. R., Lowe, D. J. & Thorneley, R. N. F. (1978) FEBS Lett. **95**, 211–213

Hageman, R. V. & Burris, R. H. (1978) Biochemistry **17**, 4117–4124

Hagen, W. R., Eady R. R. & Dunham, W. R. (1985) FEBS Lett. **189**, 250–254

Hammes, G. G. & Hurst, J. K. (1969) Biochemistry **8**, 1083–1094

Hausinger, R. P. & Howard, J. B. (1983) J. Biol. Chem. **258**, 13486–13492

Howard, J. B., Anderson, G. L. & Deits, T. L. (1985) in Nitrogen Fixation Research Progress (Evans, H. J., Bottomley, P. J. & Newton, W. E., eds.), pp. 559–565, Martinus Nijhoff, Dordrecht and Boston

Lambeth, D. O. & Palmer, G. (1973) J. Biol. Chem. **248**, 6095–6103

Lindahl, P. A., Day, E. P., Kent, T. A., Orme-Johnson, W. H. & Münck, E. (1985) J. Biol. Chem. **260**, 11160–11173

Ljones, T. & Burris, R. H. (1978) Biochemistry **17**, 1866–1872

Lowe, D. J. (1978) Biochem. J. **175**, 955–957

Lowe, D. J. & Thorneley, R. N. F. (1984*a*) Biochem. J. **224**, 877–886

Lowe, D. J. & Thorneley, R. N. F. (1984*b*) Biochem. J. **224**, 895–901

Lowe, D. J., Thorneley, R. N. F. & Smith, B. E. (1985) in Metalloproteins (Harrison, P., ed.), vol. 1, pp. 207–249, Macmillan, London

Lowery, R. G. & Ludden, P. W. (1985) in Nitrogen Fixation Research Progress (Evans, H. J., Bottomley, P. J. & Newton, W. E., eds.), p. 628, Martinus Nijhoff, Dordrecht and Boston

Morgan, T. V., Prince, R. C. & Mortenson, L. E. (1986) FEBS Lett. **206**, 4–8

Orme-Johnson, W. H. (1985) Annu. Rev. Biophys. Chem. **14**, 419–459

Saari, L. L., Pope, M. R., Murrell, S. A. & Ludden, P. W. (1986) J. Biol. Chem. **261**, 4973–4977

Smith, B. E., Thorneley, R. N. F., Yates, M. G., Eady, R. R. & Postgate, J. R. (1976) Proc. Int. Symp. Nitrogen Fixation 1st **1**, 150–161

Stephens, P. J. (1985) in Molybdenum Enzymes (Spiro, T. G., ed.) (Metal Ions in Biology Series vol. 7), pp. 117–159, Wiley–Interscience, New York

Stephens, P. J., Thomson, A. J., Dunn, J. B. R., Keiderling, T. A., Rawlings, J., Rao, K. K. & Hall, D. O. (1978) Biochemistry **17**, 4770–4778

Stephens, P. J., McKenna, C. E., McKenna, M. C., Nguyen, H. T. & Lowe, D. J. (1982) in Electron Transport and Oxygen Utilisation (Ho, C., ed.), pp. 405–509, Elsevier/North-Holland, Amsterdam

Stombaugh, N. A., Sundquist, J. E., Burris, R. H. & Orme-Johnson, W. H. (1976) Biochemistry **15**, 2633

Thorneley, R. N. F. (1974) Biochim. Biophys. Acta **333**, 487–496

Thorneley, R. N. F. (1975) Biochem. J. **145**, 391–396
Thorneley, R. N. F. & Cornish-Bowden, A. (1977) Biochem. J. **165**, 255–266
Thorneley, R. N. F. & Eady, R. R. (1973) Biochem. J. **133**, 405–408
Thorneley, R. N. F. & Lowe, D. J. (1983) Biochem. J. **215**, 393–403
Thorneley, R. N. F. & Lowe, D. J. (1984*a*) Biochem. J. **224**, 886–894
Thorneley, R. N. F. & Lowe, D. J. (1984*b*) Biochem. J. **224**, 903–909
Thorneley, R. N. F. & Lowe, D. J. (1985) in Molybdenum Enzymes (Spiro, T. G., ed.) (Metal Ions in Biology series, vol. 7), pp. 221–284, Wiley–Interscience, New York
Thorneley, R. N. F., Yates, M. G. & Lowe, D. J. (1976) Biochem. J. **155**, 137–144
Thorneley, R. N. F., Eady, R. R., Smith, B. E., Lowe, D. J., Yates, M. G., O'Donnell, M. J. & Postgate, J. R. (1979) in Nitrogen Assimilation of Plants (Hewitt, E. J. & Cutting, C. V., eds.), pp. 27–43, Academic Press, London
Walker, G. A. & Mortenson, L. E. (1973) Biochem. Biophys. Res. Commun. **53**, 904–906
Walker, G. A. & Mortenson, L. E. (1974) Biochemistry **13**, 2382–2388
Watt, G. D. (1985) in Nitrogen Fixation Research Progress (Evans, H. J., Bottomley, P. J. & Newton, W. E., eds.), pp. 585–590, Martinus-Nijhoff, Dordrecht, Boston
Watt, G. D. & Burns, A. (1977) Biochemistry **16**, 264–270
Watt, G. D. & McDonald, J. W. (1985) Biochemistry **24**, 7226–7231
Zumft, W. G., Mortenson, L. E. & Palmer, G. (1974) Eur. J. Biochem. **46**, 525–535

Received 27 January 1987/3 April 1987; accepted 19 May 1987